Hindawi
Advances in Polymer Technology
Volume 2021, Article ID 8272626, 9 pages
https://doi.org/10.1155/2021/8272626

*Research Article*

# Electrospinning and Catalytic Properties of Cyclodextrin Functionalized Polyoxymethylene (POM) Nanofibers Supported by Silver Nanoparticles

**C. Q. Zhang, Y. M. Wang, S. Z. Li, X. D. Feng, L. H. Liu, Y. Wang, and L. P. Zhao**

*Institute of Chemical and Industrial Bioengineering, Jilin Engineering Normal University, Jilin Changchun, 130052, China*

Correspondence should be addressed to C. Q. Zhang; 21991293@qq.com

Received 28 July 2021; Revised 13 October 2021; Accepted 23 October 2021; Published 13 November 2021

Academic Editor: Xinyu Zhang



A series of novel composite microfibers composed of $\beta$-cyclodextrin ($\beta$-CDs) functionalized POM (polyoxymethylene) were prepared using electrospining technology with a mixture of hexafluoroisopropanol (HFIP) and N,N-dimethylformamide (DMF) as solvent. The concentration of $\beta$-CDs with respect to the POM was varied from 0 to 50 wt.%. The effect of $\beta$-CDs content on the morphology of POM/$\beta$-CD composite microfiber was investigated. The results showed that the introduction of $\beta$-CDs reduced the surface roughness and porosity of the microfibers, and the morphology of the fibers was changed. The increase of $\beta$-CDs content from 10% to 50% has led to increased average diameter of POM/$\beta$-CD composite fiber from 2.1 $\mu$m to 6.4 $\mu$m. The mechanical properties of the blend fiber mats were further investigated. In addition, silver nanoparticles were introduced to the POM/$\beta$-CD composite microfiber matrices during electrospinning. The POM/$\beta$-CD composite fiber allows CDs to form host–guest complexes with various small molecules and macromolecules. The TEM, SEM, XRD, and XPS were utilized to characterize the prepared samples. The data suggest that Ag nanoparticles were homogeneously distributed within the POM/$\beta$-CD fibers, and no aggregation was observed. The catalytic activity of Ag nanoparticles was tracked by ultraviolet-visible (UV-vis) spectroscopy which showed excellent catalytic degradation performance of organic dyes in the presence of $NaBH_4$. The Ag/POM/$\beta$-CD mats are promising for use in waste treatment, molecular recognition, catalysis, and so on.

## 1. Introduction

Since the first description of an electrospinning setup in 1934, it has been proved to be a versatile and effective technique to produce long and continuous fibers. In a typical electrospinning process, a high voltage is applied to eject a polymer jet, and a nanofiber mat is eventually formed as the solvent evaporates. The structure of electrospun fiber can be easily tuned through the precise control of various electrospinning parameters, which provides great flexibility for modifying the surface morphology of electrospun film, and offers the fiber materials with high specific surface area, high length-width ratio, high porosity, and others. Following the development of the electrospinning research, most of the studies have been focused on controlling the surface morphology of electrospun films in various applications. Furthermore, some works demonstrated the successful incorporation of functional molecules into nanofibers to form resulting composites with excellent chemical and physical properties [1–3]. These functional nanofibers have a very wide range of applications in optoelectronics, sensor technology, catalysis, filtration, medicine, and other fields [4–6].

Polyoxymethylene (POM) is a versatile engineering plastic with high crystalline composition. Since the start of its commercial production in the 1960s, the use of POM has spread rapidly in the polymer industry, and various processes have been successfully developed for processing POM. Nowadays, molded and extruded POM parts with high stiffness, low

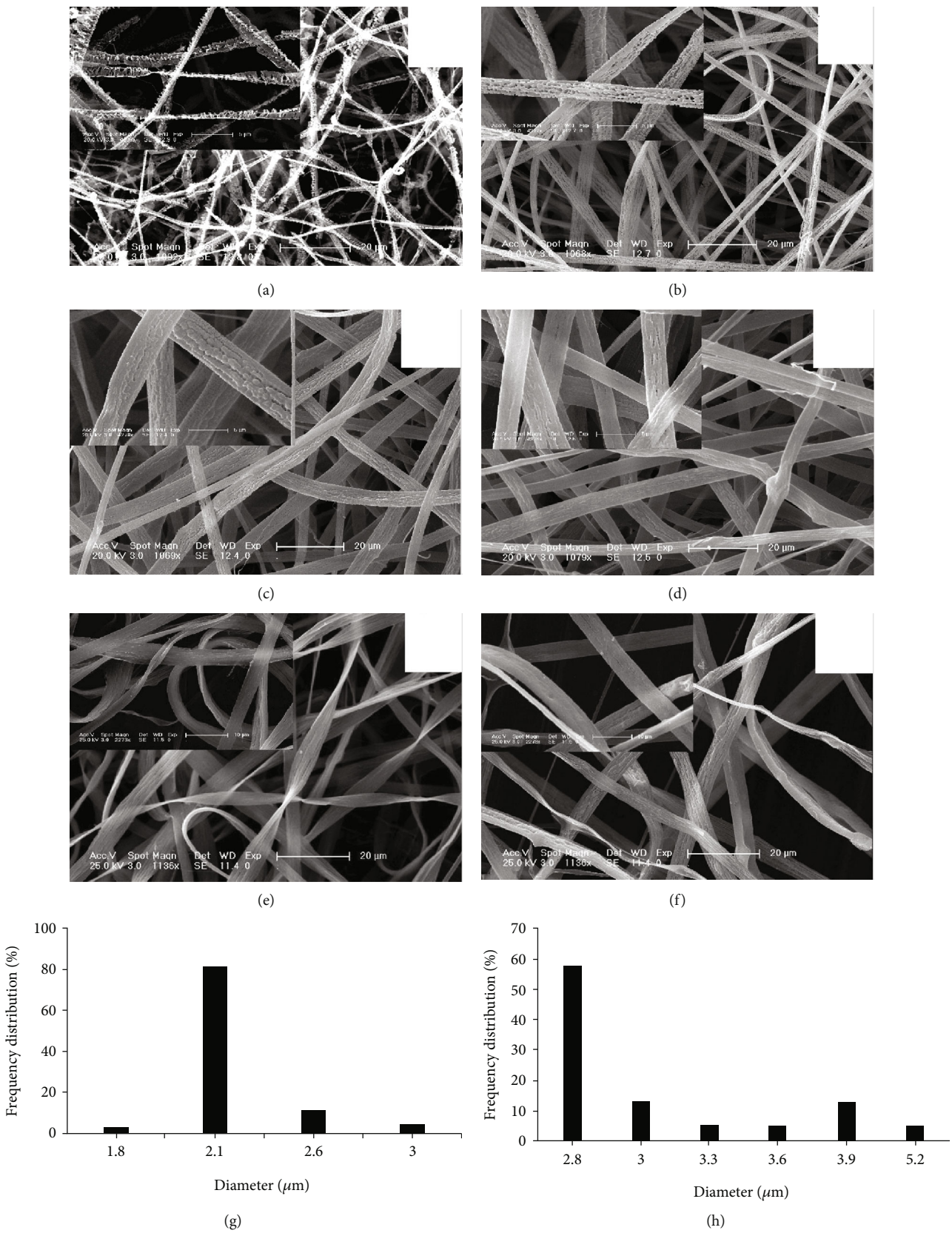


Figure 1: Continued.

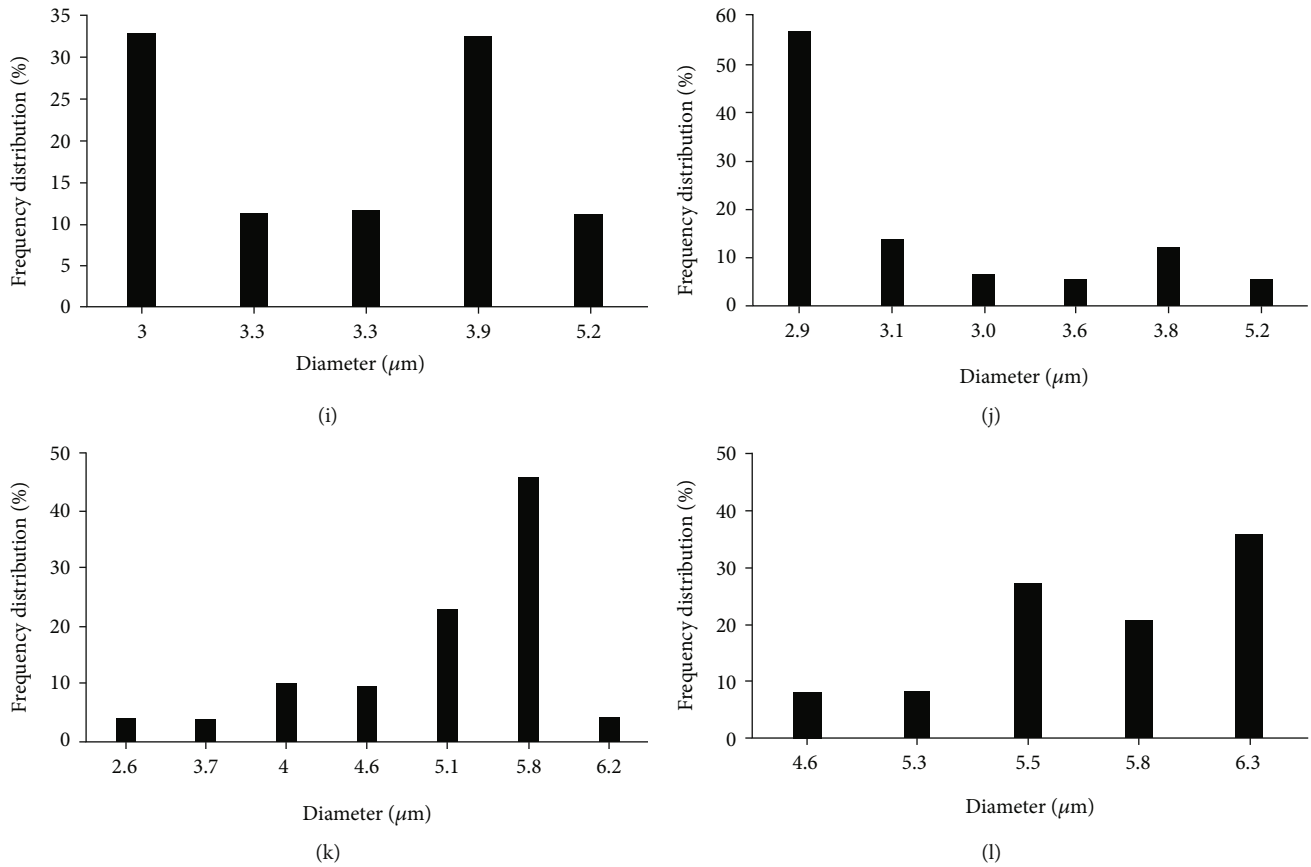


Figure 1: Scanning electron micrographs and frequency distribution of the fiber diameters of the electrospun POM/$\beta$-CD microfibers with different contents of $\beta$-CDs (a, g) 0 wt.% $\beta$-CDs, (b, h) 10 wt.% $\beta$-CDs, (c, i) 20 wt.% $\beta$-CDs, (d, j) 30 wt.% $\beta$-CDs, (e, k) 40 wt.% $\beta$-CDs, and (f, l) 50 wt.% $\beta$-CDs.

friction, and excellent dimensional stability are used extensively in appliances, machinery, instruments, automobile, marine, aviation, building, and agriculture. Various processes, including injection molding, extrusion, blow molding, and rolling mill, have been successfully developed for processing POM. However, due to poor solubility of POM in common solvents, researches on electrospinning are rarely reported, and the progress of relevant scientific research is slow [7–10].

Cyclodextrins (CDs) are a family of cyclic oligosaccharide with cyclic molecular structure, and they are composed of $\alpha$ (1,4) linked cyclic pyridoglycan units. The most common natural CDs contain 6, 7, or 8 glucopyranose units in the cycle and are named as $\alpha$-CD, $\beta$-CD, and $\gamma$-CD, respectively. The CDs are considered as one of the super molecules pioneers with wide applications in different fields, such as host–guest interaction, molecular recognition, drug delivery, enzyme catalysis, foods, cosmetics, and pesticides. The functionalization of microfibers/nanofibers with cyclodextrins will provide unique properties to traditional composite fibers. For instance, micro/nanofibers have potential to be used for filtering tiny particles as well as serving as barriers for liquid/vapor penetration due to the large surface area of nanoporous structure [11–14]. In addition, the hydrophobic cavity of CDs allows them to form host–guest complexes with various small molecules and macromolecules. In our previous study, we showed the doping of $\beta$-CDs into electrospinning fibers and further studied the doping mechanism of $\beta$-CDs with polymers as well as the utilization of resulting composite fibers as carrier to catalyze organic reactions [15–17]. With the development of composite photocatalyst research, the carrier of photocatalyst has become an important factor restricting the development of photocatalyst materials. The recovery of catalytic materials without causing secondary environmental pollution has also become a focus for scientists. On the other hand, the catalytic efficiency will be greatly improved if the catalytic material can capture pollutants and photocatalysis at the same time. POM microfiber is a well-investigated type of composite microfiber with excellent tensile strength to be used as framework to support $\beta$-CDs. The hydrophobic cavity of CDs allows them to form host–guest complexes with Ag nanoparticles in POM [18–21]. And to the best of our knowledge, the preparation of Ag/POM/$\beta$-CD composite microfiber matrices using electrospinning has not yet been reported.

In this study, we reported the fabrication of POM/$\beta$-CD composite microfiber matrices with well-dispersed silver nanoparticles (Ag NPs) by using a simple electrospinning method. POM/$\beta$-CD blends containing 0–50 wt.% $\beta$-CDs were electrospun using solvent mixture of

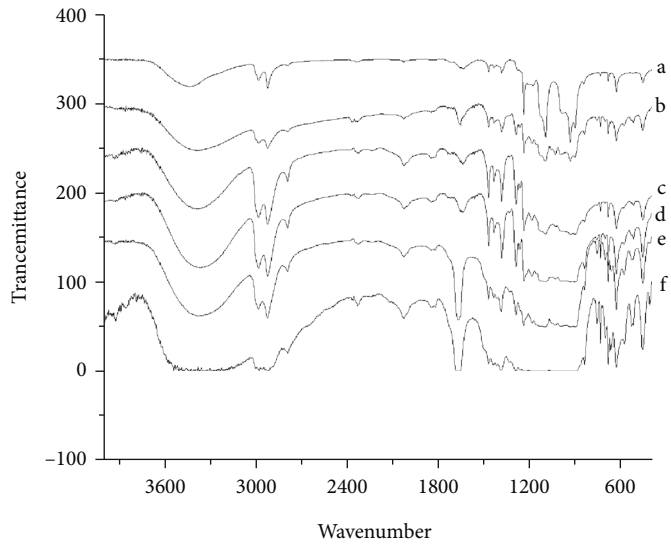


Figure 2: FTIR spectrum of POM/$\beta$-CD microfibers film with different content of $\beta$-CDs (a) 0 wt.% $\beta$-CDs, (b) 10 wt.% $\beta$-CDs, (c) 20 wt.% $\beta$-CDs, (d) 30 wt.% $\beta$-CDs, (e) 40 wt.% $\beta$-CDs, and (f) 50 wt.% $\beta$-CDs.

hexafluoroisopropanol (HFIP) and N,N-dimethylformamide (DMF). The effect of $\beta$-CDs content on POM/$\beta$-CD composite morphology was discussed. The TEM, SEM, XRD, and XPS were employed to characterize the prepared samples. The catalytic degradation performance for organic dyes in the presence of $NaBH_4$ was discussed and tracked by ultraviolet-visible (UV-vis) spectroscopy. The composite microfiber matrices showed excellent catalytic activity and are promising for use in waste treatment, molecular recognition, catalysis, and so on.

## 2. Materials and Methods

*2.1. Materials.* POM was a commercial grade powder (M 90) without any additives and was supplied by Dongguan HengTong Plastic Materials Co., Ltd. (China). Silver nitrate ($AgNO_3$) was purchased from Sinopharm Medicine Holding Shenyang Co. Ltd (China). Sodium borohydride ($NaBH_4$), methylene blue trihydrate (MB), hexafluoroisopropanol (HFIP), N,N-dimethylformamide (DMF), and $\beta$-CDs were supplied by Beijing Chemicals, Co. (China). In all experiments, the chemicals were analytical grade, and all reagents were used as received without any further purification.

## 3. Electrospinning

*3.1. Preparation of POM/$\beta$-CD Composite Microfiber by Electrospinning.* POM (8 wt.%) was first dissolved in solvent mixture of HFIP/DMF with ratio of 98 : 2 (w/w). Different amounts of $\beta$-CDs (0 wt.%, 10 wt.%, 20 wt.%, 30 wt.%, 40 wt.%, 50 wt.%) were added to the prepared POM solutions at room temperature to obtain different concentrations of precursor solutions. The precursor solutions were stirred at room temperature for 12 h. After that, the solution obtained was added into a plastic syringe with internal diameter of pinhead at 0.8 nm, the pinhead was connected

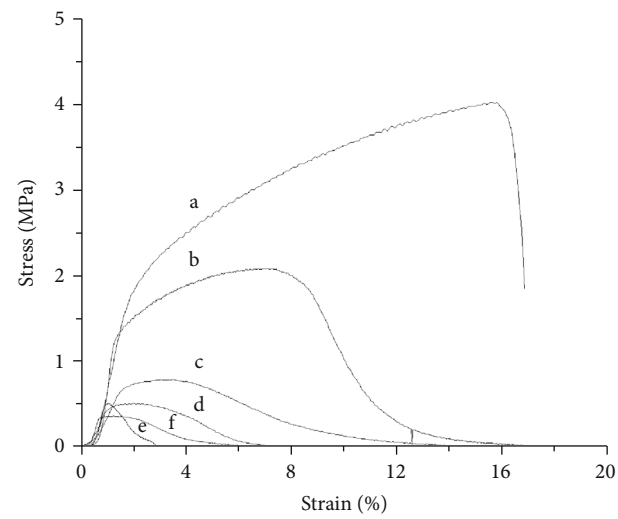


Figure 3: Stress-strain curve of POM/$\beta$-CD microfiber films with different contents of $\beta$-CDs: (a) 0 wt.% $\beta$-CDs, (b) 10 wt.% $\beta$-CDs, (c) 20 wt.% $\beta$-CDs, (d) 30 wt.% $\beta$-CDs, (e) 40 wt.% $\beta$-CDs, and (e) 50 wt.% $\beta$-CDs.

to a 15 kv high-voltage electrode, the distance between capillary syringe and substrate electrode was 15 cm, and the feed rate of the solution was 2 ml/h controlled through a syringe pump. The whole electrospinning process was performed at 20°C.

*3.2. Preparation of Ag/POM/$\beta$-CD Composite Microfibers by Electrospinning.* Silver ions were introduced into the above six precursor solutions. The solutions were stirred in the dark at 0°C for about 12 h. A series of $AgNO_3$/POM/$\beta$-CD composite microfibers film were further obtained by electrospinning. The electrospinning condition was the same as formulating POM/$\beta$-CD composite microfibers. Finally, each of the films was immersed into $NaBH_4$ (10 ml,

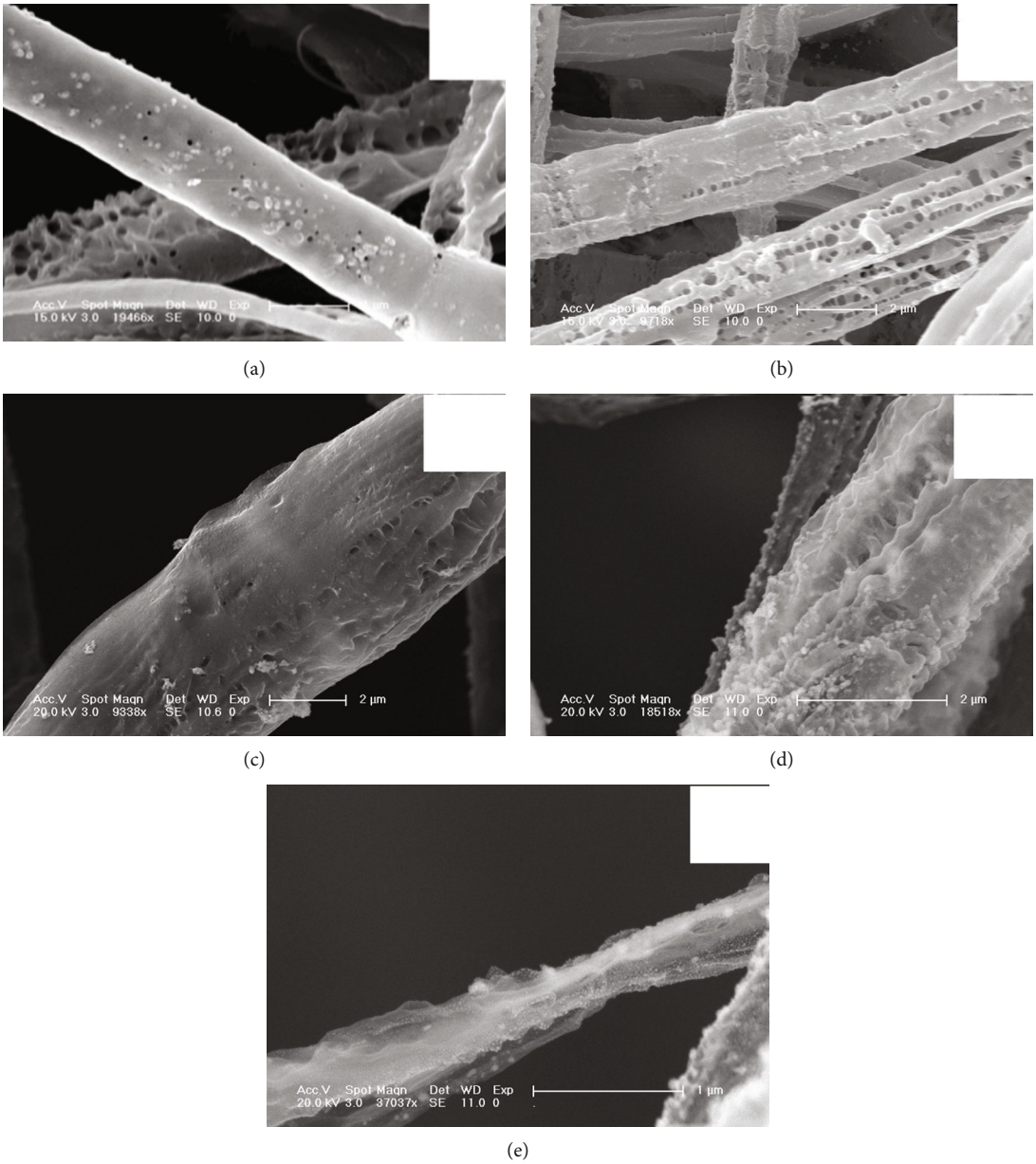


Figure 4: Scanning electron micrographs of the electrospun Ag/POM/$\beta$-CD microfibers with different contents of $\beta$-CDs: (a) 10 wt.% $\beta$-CDs, (b) 20 wt.% $\beta$-CDs, (c) 30 wt.% $\beta$-CDs, (d) 40 wt.% $\beta$-CDs, and (e) 50 wt.% $\beta$-CDs.

0.5 wt.%) aqueous solution for 5 minutes to complete the reduction of silver cations. The color of the film changed from white to brown due to the reaction occurrence.

*3.3. Catalytic Activity of Ag/POM/$\beta$-CD Composite Microfibers.* The catalytic activity of the Ag/POM/$\beta$-CD composite nanofiber was analyzed following the procedure as described in the literature [22, 23]. For a model reaction, a piece of Ag/POM/$\beta$-CD composite microfiber film (5 mg) was homogeneously unfolded and soaked into a MB dye aqueous solution ($2 \times 10^{-5}$ mol/l, 2 ml), and aqueous $NaBH_4$ (0.1 mol/l, 1 ml) was then injected into the solution rapidly with constant magnetic stirring. The entire reduction reaction experiment was conducted under nitrogen. It can be clearly observed that the intensity of blue color of the reaction mixture decreased gradually and turned colorless at the end. The absorbance value of MB feature at 665 nm, monitored with UV-vis spectrometer, was used as an indication of catalytic activity of silver particles.

## 4. Results and Discussion

*4.1. Morphology of POM/$\beta$-CD Microfibers.* To characterize the morphology of the composite microfiber, SEM measurements were performed. When $\beta$-CDs content was greater than 50 wt.%, the viscosity of precursor solution became so

high that the electrospinning was difficult to maintain. Therefore, only POM/$\beta$-CD blends containing 0-50 wt.% $\beta$-CDs were investigated. Figures 1(a)–1(f) show the fiber morphology. The frequency distribution of fiber diameters shown in Figures 1(g)–1(l) was randomly measured from SEM photographs. It can be seen that the morphology of fibers changed drastically when the concentration of $\beta$-CDs varied. Figures 1(a) and 1(g) demonstrate that pure POM fibers are porous with an average pore size of 2.1 $\mu$m. Statistical analysis based on more than 100 fibers of each sample indicated that the introduction of $\beta$-CDs leads to increased average fiber diameter from 2.1 $\mu$m to 6.4 $\mu$m, and the roughness and porosity of microfiber surface are decreased. The physical properties of the precursor solution play an important role in the electrospinning process, and the concentration and solvent are the most effective parameters for controlling the fiber morphology. For instance, microporous structure is frequently obtained when volatile solvents or low concentration solutions are used in electrospinning. POM has poor solubility in common solvents but HFIP, and the HFIP solvent evaporation rate is faster when mixed with POM. This may be related to the semicrystalline nature of POM and the difference in solvent-polymer interaction. The ripple features observed on RF electrospun fibers were attributed to the occurrence of phase separation during solvent evaporation process due to high vapor pressure of HFIP solvent. The use of lower electrospinning voltage delayed polymer ejection and thus facilitated the evaporation of HFIP during the jet flight. In addition, the addition of $\beta$-CDs to precursor solution has increased the concentration and viscosity of the solution, which eventually led to decreased surface roughness and porosity of microfibers after electrospinning.

*4.2. FTIR.* Figure 2 shows the FTIR spectra of POM/$\beta$-CD microfibers with different concentrations of $\beta$-CDs. The spectrum of pure POM (Figure 2(a)) demonstrates a peak at 3444 $cm^{-1}$, attributed to –OH band stretching on POM structure. At the same time, when the contents of $\beta$-CDs increased in POM/$\beta$-CD composite microfibers, the –OH band position shifted from 3444 $cm^{-1}$ to 3387 $cm^{-1}$ with gradual increase of band intensity in matrix. This phenomenon can be explained by the overlapping of -OH band present in $\beta$-CD and POM molecules in this region.

*4.3. Mechanical Properties of POM/$\beta$-CD Composite Microfiber Sheets.* Typical stress-strain curve obtained by stretching test was used to evaluate the mechanical properties of the electrospun micro/nanofiber films (Figure 3). Based on the mechanical data, it can be seen that the elongation and tensile strength of POM/$\beta$-CDs were slightly reduced with the increase of $\beta$-CDs content. It can be explained by the cyclic structure of CDs consisting of $\alpha$-(1, 4-) linked glucopyranose units with a toroid-shaped structure, which ultimately resulted in decreased mechanical properties of composite microfibers. The mechanical intensity of prepared POM/$\beta$-CDs, though reduced, was still comparable to other polymer fibers' such as PAN.

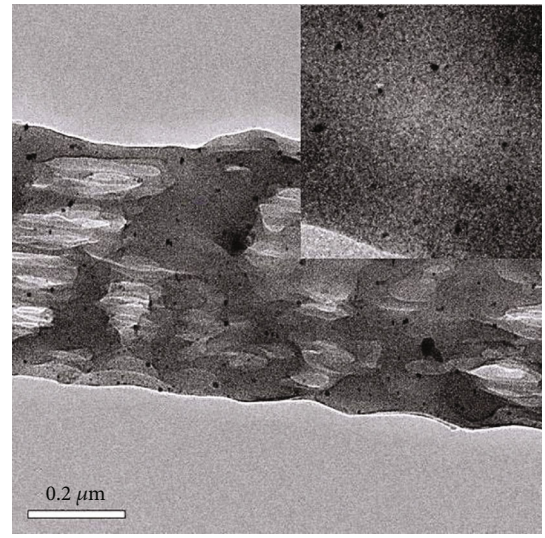


Figure 5: TEM of the POM/$\beta$-CD microfibers' film 30 wt.% $\beta$-CDs.

*4.4. Morphology of Ag/POM/$\beta$-CD Microfibers.* Figure 4 shows the SEM images of Ag/POM/$\beta$-CD microfibers. The SEM images clearly demonstrated that individual Ag NPs were homogeneously distributed within the fibers, and no aggregation was observed. The amount of Ag NPs present on fibers increased with constant addition of $\beta$-CDs in the fiber film. The hydrophobic cavity of $\beta$-CDs allows them to form effective host–guest complexes with Ag NPs, thus contributed to increased particle inclusion and improved homogeneity of Ag NPs as the concentration of $\beta$-CDs increases in precursor solution.

*4.5. TEM of Ag/Ag/POM/$\beta$-CD Microfibers.* In the circumstance when $\beta$-CDs content was higher than 30 wt.%, the mechanical properties of the fiber films were low, which may restrict the range of applications. Therefore, only the POM/$\beta$-CD blends containing 30 wt.% $\beta$-CDs were investigated by TEM and XRD. The TEM image is shown in Figure 5, and the dark spots on the nanofibers are Ag nanoparticles. It can be seen that the Ag nanoparticles have dispersed homogenously in the nanofiber. At the same time, core sheath structure was observed. The core is not exactly located at the center of fibers. The sheath comes from $\beta$-CDs structure which forms a membrane outside the POM. Since that pure POM is extremely sensible to electron beam, it is very difficult to observe the fibers closely and carefully. Therefore, the TEM image cannot be taken without the layer of $\beta$-CDs outside. In addition, the formation of core/sheath structure depends on both thermodynamic and kinetic factors [2]. Bognitzki et al. reported the major component forms the core [24]. In this work, as the major component in our electrospinning solution, POM is identified as the core part.

*4.6. XRD of Ag/Ag/POM/$\beta$-CD Microfibers.* Figure 6 shows the XRD spectrum of Ag/POM/$\beta$-CD microfiber film with 30 wt.% $\beta$-CDs. The strong diffraction peaks with $2\theta$ values of 38.1°, 44.4°, 66.4°, and 77.4° correspond to the (111),

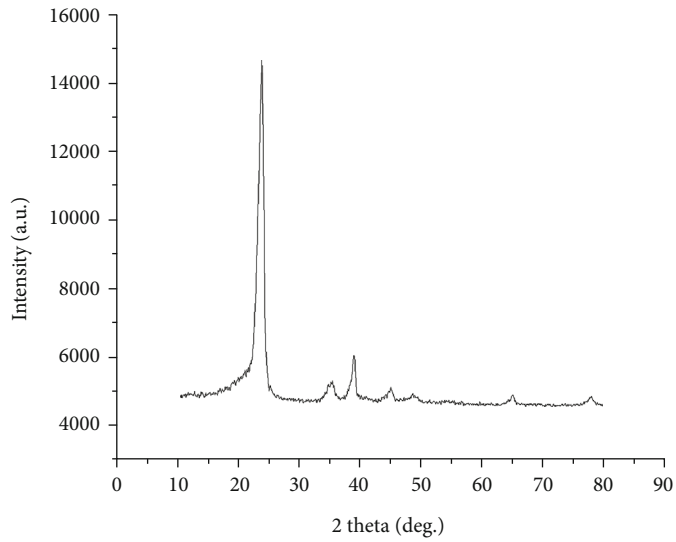


Figure 6: XRD spectrum of Ag/POM/$\beta$-CD microfibers film with 30 wt.% $\beta$-CDs.

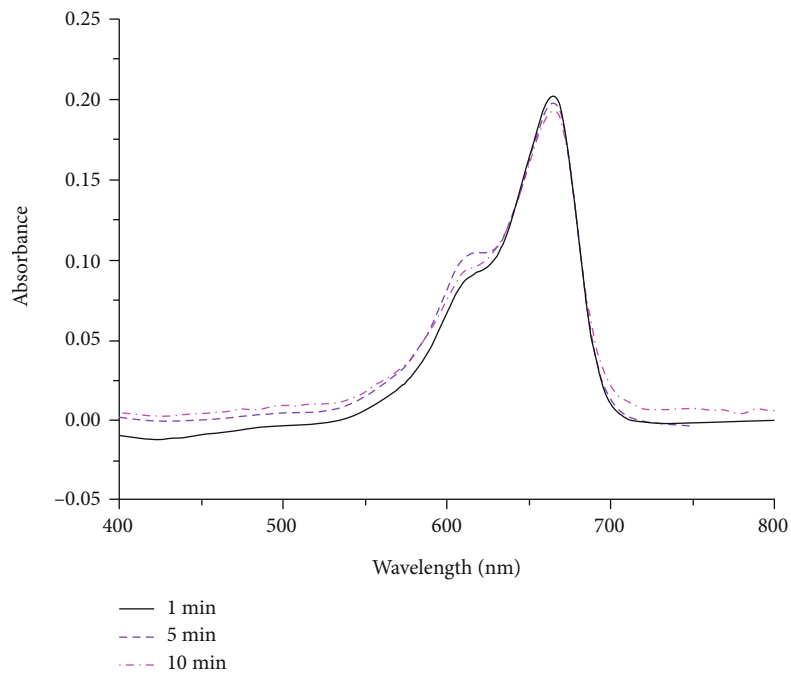


Figure 7: UV–vis spectra of a mixture of methylene blue dye ($2 \times 10^{-5}$ M, 2 ml aqueous solution) and reducing agent $NaBH_4$ (0.1 M, 1 ml) without silver particles.

(200), (220), and (311) crystal faces of the fcc crystalline silver, respectively [25]. The result indicates that silver nanoparticles are present in the form of face-centered cubic (fcc) crystal on Ag/POM/$\beta$-CD nanofiber film.

*4.7. Catalytic Performance of Ag/POM/$\beta$-CD Microfibers.* Methylene blue is a cationic thiazine dye, the oxidized form of aqueous solution is dark blue, and the reductive form of aqueous solution is colorless. Sodium borohydride was used as a reducing agent in the catalytic degradation reaction system of methylene blue. Although sodium borohydride is a strong reducing agent, the aqueous solution of sodium borohydride does not effectively reduce methylene blue because of the significant REDOX potential difference between the dye and sodium borohydride [22, 23].

For comparison, a blank test is conducted with a mixture of MB dye and $NaBH_4$ reducing agent without silver particles. Within 30 min, there is no decrease of absorbance of MB at 665 nm monitored by UV (Figure 7). This redox reaction will not occur unless there is catalyst present in the

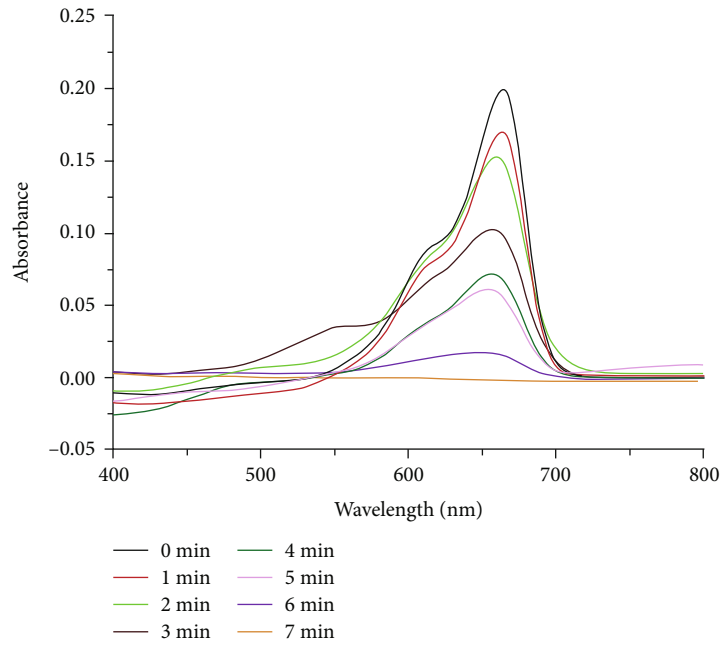


Figure 8: Ultraviolet–visible (UV–vis) spectra of a mixture of methylene blue dye ($2 \times 10^{-5}$ M, 2 ml aqueous solution) and reducing agent $NaBH_4$ (0.1 M, 1 ml) in the presence of Ag/POM/$\beta$-CD microfibers' film with different reaction times.

reaction medium. When the experiment was carried out in the presence of Ag/POM/$\beta$-CD microfibers' film as catalyst, the color of the solution is changed significantly from blue to colorless. The ultraviolet–visible (UV–vis) spectroscopy was used to track the progress of the reaction. It can be seen in Figure 8 that the absorbance feature of MB at 665 nm gradually decreases with reaction time, which indicates that the catalytic reduction of MB has proceeded successfully, and no deactivation or poisoning of the catalyst was observed.

## 5. Conclusions

We have shown that a series of novel POM/$\beta$-CD composite fibers were prepared via electrospinning. The variation of $\beta$-CDs content can impact the morphology of final composite film. The introduction of $\beta$-CDs decreases surface roughness and porosity and increases the average diameter of fibers significantly. The mechanical properties of the blend fiber mats were also investigated. It was found that the elongation and tensile strength of POM/$\beta$-CDs were slightly reduced with the increased $\beta$-CDs content, but was still comparable to other polymer micro/nanofibers. Furthermore, Ag/POM/$\beta$-CD composite microfiber matrices were electrospun, the SEM, TEM, and X-ray diffraction suggest that the individual Ag nanoparticles were homogeneously distributed within the fibers, and no aggregation was observed in Ag/POM/$\beta$-CDs.

## Data Availability

Data are openly available in a public repository that issues datasets with DOIs.

## Conflicts of Interest

The authors declare that they have no conflicts of interest.

## Acknowledgments

We thank the Doctoral Research Start-Up Fund from Jilin Engineering Normal University (No. BSKJ202003).

## References

[1] Y. C. Ahn, S. K. Park, G. T. Kim et al., "Development of high efficiency nanofilters made of nanofibers," *Current Applied Physics*, vol. 6, no. 6, pp. 1030–1035, 2006.

[2] M. Wei, B. Kang, C. Sung, and J. Mead, "Core-sheath structure in electrospun nanofibers from polymer blends," *Macromolecular Materials and Engineering*, vol. 291, no. 11, pp. 1307–1314, 2006.

[3] K. Tan and S. K. Obendorf, "Fabrication and evaluation of electrospun nanofibrous antimicrobial nylon 6 membranes," *Journal of Membrane Science*, vol. 305, no. 1-2, pp. 287–298, 2007.

[4] R. Barhate and S. Ramakrishna, "Nanofibrous filtering media: filtration problems and solutions from tiny materials," *Journal of Membrane Science*, vol. 296, no. 1-2, pp. 1–8, 2007.

[5] M. Bognitzki, W. Czado, T. Frese et al., "Nanostructured fibers via electrospinning," *Advanced Materials*, vol. 13, no. 1, pp. 70–72, 2001.

[6] Y. Z. Zhang, Z. M. Huang, X. J. Xu, C. T. Lim, and S. Ramakrishna, "Preparation of core–shell structured PCL-r-gelatin bi-component nanofibers by coaxial electrospinning," *Chemistry of Materials*, vol. 16, no. 18, pp. 3406–3409, 2004.

[7] Y. Li, T. Xie, and G. Yang, "Studies on novel composites of polyoxymethylene/polyamide 6," *Journal of Applied Polymer Science*, vol. 99, no. 1, pp. 335–339, 2006.

[8] S. Lee and S. Kay Obendorf, "Developing protective textile materials as barriers to liquid penetration using melt-electrospinning," *Journal of Applied Polymer Science*, vol. 102, no. 4, pp. 3430–3437, 2006.

[9] P. Peng, Y. Z. Chen, Y. F. Gao, J. Yu, and Z. X. Guo, "Phase morphology and mechanical properties of the electrospun polyoxymethylene/polyurethane blend fiber mats," *Journal of Polymer Science Part B: Polymer Physics*, vol. 47, no. 19, pp. 1853–1859, 2009.

[10] F. X. Espinach, L. A. Granda, Q. Tarrés, J. Duran, P. Fullana-i-Palmer, and P. Mutjé, "Mechanical and micromechanical tensile strength of eucalyptus bleached fibers reinforced polyoxymethylene composites," *Composites Part B Engineering*, vol. 116, no. 1, pp. 333–339, 2017.

[11] S. Tingry, C. Innocent, S. Touil, A. Deratani, and P. Seta, "Carbon paste biosensor for phenol detection of impregnated tissue: modification of selectivity by using $\beta$-cyclodextrin-containing PVA membrane," *Materials Science and Engineering: C*, vol. 26, no. 2–3, pp. 222–226, 2006.

[12] A. Sergey and J. F. Nepogodiev, "Cyclodextrin-based Catenanes and Rotaxanes," *Chemical Reviews*, vol. 98, no. 5, pp. 1959–1976, 1998.

[13] G. Wenz, "Cyclodextrins as building blocks for supramolecular structures and functional units," *Angewandte Chemie International Edition in English*, vol. 33, no. 8, pp. 803–822, 1994.

[14] M. Bouzitoun, R. Mlika, H. Gam, H. B. Ouada, M. Majdoub, and H. Sfihi, "A non-water-soluble modified $\beta$-cyclodextrin for sensitive electrode," *Materials Science and Engineering: C*, vol. 26, no. 2–3, pp. 481–485, 2006.

[15] J. Bai, Q. B. Yang, M. Y. Li, C. Q. Zhang, and L. Yiaoxian, "Synthesis of poly(_N_ -vinylpyrrolidone)/$\beta$-cyclodextrin composite nanofibers using electrospinning techniques," *Journal of Materials Processing Technology*, vol. 208, no. 1–3, pp. 251–254, 2008.

[16] C. Q. Zhang, Q. B. Yang, N. Q. Zhan et al., "Silver nanoparticles grown on the surface of PAN nanofiber: preparation, characterization and catalytic performance," *Colloids and Surfaces A: Physicochemical and Engineering Aspects.*, vol. 362, no. 1–3, pp. 58–64, 2010.

[17] J. Bai, Q. B. Yang, M. Y. Li, S. Wang, C. Q. Zhang, and Y. X. Li, "Preparation of composite nanofibers containing gold nanoparticles by using poly(_N_ -vinylpyrrolidone) and $\beta$\- cyclodextrin," *Materials Chemistry and Physics*, vol. 111, no. 2–3, pp. 205–208, 2008.

[18] M. Shirzadi-Ahodashti, Z. Hashemi, Y. Mortazavi, K. Khormali, S. Mortazavi-Derazkola, and M. A. Ebrahimzadeh, "Discovery of high antibacterial and catalytic activities against multi-drug resistant clinical bacteria and hazardous pollutants by biosynthesized of silver nanoparticles using Stachys inflata extract (AgNPs@SI)," *Colloids and Surfaces A: Physicochemical and Engineering Aspects*, vol. 617, no. 126, p. 383, 2021.

[19] B. Kim, W. C. Song, S. Y. Park, and G. Park, "Green synthesis of silver and gold nanoparticles via Sargassum serratifolium extract for catalytic reduction of organic dyes," *Catalysts*, vol. 11, no. 3, pp. 347–360, 2021.

[20] M. A. Polinarski, A. L. B. Beal, F. E. B. Silva et al., "New perspectives of using chitosan, silver, and chitosan–silver nanoparticles against multidrug-resistant bacteria," *Particle & Particle Systems Characterization*, vol. 38, no. 4, article 2100009, 2021.

[21] D. Paul, D. Sachan, and G. Das, "Silver nanoparticles embedded on in-vitro biomineralized vaterite: a highly efficient catalyst with enhanced catalytic activity towards 4-Nitrophenol reduction," *Molecular Catalysis*, vol. 504, pp. 2468–8231, 2021.

[22] S. K. Ghosh, S. Kundu, M. Mandal, and T. Pal, "Silver and gold nanocluster catalyzed reduction of methylene blue by arsine in a micellar medium," *Langmuir*, vol. 18, no. 23, pp. 8756–8760, 2002.

[23] N. Gupta, H. P. Singh, and R. K. Sharma, "Metal nanoparticles with high catalytic activity in degradation of methyl orange: an electron relay effect," *Journal of Molecular Catalysis A: Chemical*, vol. 335, no. 1-2, pp. 248–252, 2011.

[24] T. F. Mikhail Bogntizki, S. Martin, and G. Reas, "Preparation of fibers with nanoscaled morphologies: electrospinning of polymer blends," *Polymer Engineering and Scienc*, vol. 41, no. 6, pp. 982–989, 2001.

[25] Y. Z. Wang, Y. X. Li, S. T. Yang et al., "A convenient route to polyvinyl pyrrolidone/silver nanocomposite by electrospinning," *Nanotechnology*, vol. 17, no. 13, pp. 3304–3307, 2006.